Revealing the large-scale network organization of growth hormone-secreting cells

Xavier Bonnefont*†, Alain Lacampagne†‡, Angela Sanchez-Hormigo*†, Elodie Fino*§, Audrey Creff*¶, Marie-Noelle Mathieu*, Sébastien Smallwood*‖, Danielle Carmignac**, Pierre Fontanaud*, Pierre Travo††, Gérard Alonso*, Nathalie Courtois-Coutry*, Steve M. Pincus‡‡, Iain C. A. F. Robinson**, and Patrice Mollard*§§

*Department of Endocrinology, Institute of Functional Genomics, Centre National de la Recherche Scientifique, Unité Mixte de Recherche 5203, Institut National de la Santé et de la Recherche Médicale U661, Universities of Montpellier 1 and 2, 141 Rue de la Cardonille, 34094 Montpellier Cedex 05, France; ‡Institut National de la Santé et de la Recherche Médicale U637, Centre Hospitalier Universitaire Arnaud de Villeneuve, 34295 Montpellier Cedex 05, France; **Division of Molecular Neuroendocrinology, National Institute of Medical Research, The Ridgeway, Mill Hill, London NW7 1AA, United Kingdom; ††Montpellier RIO Imaging, Centre de Recherches de Biochimie Macromoléculaire, Formation de Recherche en Evolution 2593, Centre National de la Recherche Scientifique, 1919 Route de Mende, 34293 Montpellier Cedex 05, France; and ‡‡990 Moose Hill Road, Guilford, CT 06437

Communicated by Roger Guillemin, The Salk Institute for Biological Studies, La Jolla, CA, September 23, 2005 (received for review May 7, 2005)

Pituitary growth hormone (GH)-secreting cells regulate growth and metabolism in animals and humans. To secrete highly ordered GH pulses (up to 1,000-fold rise in hormone levels *in vivo*), the pituitary GH cell population needs to mount coordinated responses to GH secretagogues, yet GH cells display an apparently heterogeneous scattered distribution in 2D histological studies. To address this paradox, we analyzed in 3D both positioning and signaling of GH cells using reconstructive, two-photon excitation microscopy to image the entire pituitary in GH-EGFP transgenic mice. Our results unveiled a homologous continuum of GH cells connected by adherens junctions that wired the whole gland and exhibited the three primary features of biological networks: robustness of architecture across lifespan, modularity correlated with pituitary GH contents and body growth, and connectivity with spatially stereotyped motifs of cell synchronization coordinating cell activity. These findings change our view of GH cells, from a collection of dispersed cells to a geometrically connected homotypic network of cells whose local morphology and connectivity can vary, to alter the timing of cellular responses to promote more coordinated pulsatile secretion. This large-scale 3D view of cell functioning provides a powerful approach to identify and understand other networks of endocrine cells that are thought to be scattered *in situ*. Many dispersed endocrine systems exhibit pulsatile outputs. We suggest that cell positioning and associated cell–cell connection mechanisms will be critical parameters that determine how well such systems can deliver a coordinated secretory pulse of hormone to their target tissues.

biological rhythms | endocrinology | systems biology | connectivity | calcium

Many endocrine responses are episodic in nature. One of the best characterized responses is the release of growth hormone (GH) from GH-secreting cells (the major population of endocrine cells in the pituitary gland), which regulates body growth and metabolism (1). At present, functional assessment of GH cells is based on cell numbers and activities (1, 2). However, this current concept faces a paradox. The GH cell population in the pituitary produces massive GH pulses in response to physiological needs (up to a thousand-fold increase in GH concentration) (3–5) whereas the pulses are much smaller when GH cells are studied out of their tissue context (6). The functional organization of GH cells that might explain the coordinated responses of the thousands of individual GH cells located within the gland is, however, poorly understood. No converging view has emerged from previous histological studies that showed most pituitary endocrine cell types heterogeneously distributed and scattered throughout the mammalian gland parenchyma in what seemed to be a random mosaic fashion (2, 7).

To overcome the difficulty of interpreting 3D-like representations from serial thin tissue sections, we directly visualized and monitored activities of identified pituitary cells in the intact tissue. The production of GH-GFP transgenic mice made it possible to identify and locate the 3D position of every identified GH cell in the pituitary gland, by using a combination of two-photon excitation microscopy and off-line reconstruction and analysis, and to study activity in multiple living GH cells, identified in 3D space. Thus, we discovered a functional GH cell network that wired the whole gland and underwent geometry-driven changes that correlated with the activity of the GH axis.

Methods

Multiphoton Imaging of GH-EGFP Pituitaries. In fixed pituitaries, fluorescence images were acquired in *x–y* mode with a Zeiss LSM 510 NLO confocal system (×25 oil immersion, numerical aperture (N.A.) = 0.8). Multiphoton excitation was achieved with a 5-W Mira/Verdi pulsed TI/sapphire laser (Coherent, Orsay, France) tuned at 840 nm (pulse duration of ≈150 fs and bandwidth of ≈8 nm). The emitted fluorescence was recorded at 520 nm (8, 9). In some experiments, high-pressure cardiac perfusion was performed before tissue fixation peroxidase immunostaining and electron microscopy as described (10).

Hormone Release Assays, Calcium Recordings, and Analysis. Mouse GH and EGFP in either pituitary or cell incubation medium were assayed by RIA as described (11), by using mouse reagents kindly provided by the National Institute of Diabetes and Digestive and Kidney Diseases (Bethesda). Cytosolic calcium was monitored in GH-EGFP cells loaded with the fluorescent calcium dye fura-2 as reported (11). Custom-made software in IGOR PRO (WaveMetrics, Lake Oswego, OR) was used to measure the linear correlation (Pearson *R*) between all pairs of GH-EGFP cells. To test whether motifs of gross synchrony between GH-EGFP cells occurred, we

Conflict of interest statement: No conflicts declared.

Freely available online through the PNAS open access option.

Abbreviations: GH, growth hormone; GHRH, GH-releasing hormone; V/S, volume-to-surface.

†X.B., A.L., and A.S-H. contributed equally to this work.

§Present address: Laboratoire de Neurobiologie Pharmacologique, Institut National de la Santé et de la Recherche Médicale U-114, Collège de France, 11 place Marcelin Berthelot, 75005 Paris, France.

¶Present address: Département d'Ecophysiologie Végétale et de Microbiologie, Laboratoire de Biologie du Développement des Plantes, Commissariat à l'Energie Atomique (CEA) Cadarache, 13108 Saint Paul Lez Durance, France.

‖Present address: Centre National de la Recherche Scientifique, Unité Mixte de Recherche 5123, University Lyon 1, 43 boulevard du 11 Novembre 1918, 69622 Villeurbanne Cedex, France.

§§To whom correspondence should be addressed at: Department of Endocrinology, Institute of Functional Genomics, 141 Rue de la Cardonille, 34094 Montpellier Cedex 05, France. E-mail: patrice.mollard@igf.cnrs.fr.

www.pnas.org/cgi/doi/10.1073/pnas.0508202102

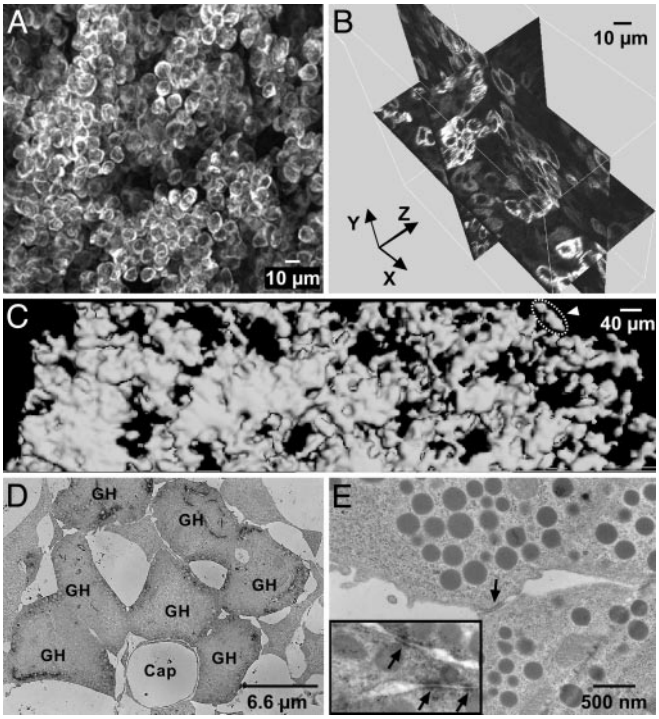

Fig. 1. Three-dimensional continuum of the GH cell population. (*A*) Two-photon image stack (70-μm thickness) taken from an intact GH-GFP mouse pituitary. For a sample movie, see Movie 1. (*B*) Shown is 3D orthogonal slicing of a two-photon image stack (80-μm thickness). (*C*) Surface rendering of GH-GFP cell contours from four juxtaposed two-photon image stacks (30-μm thickness) covering the distance from the dorsal (left) to the ventral (right) sides of a GH-GFP pituitary. The cell contours were almost all in close contact to each other (automatic detection procedure), except a small cell group (surrounded by a dashed line, arrowhead). (*D* and *E*) Mice were fixed with glutaraldehyde after a procedure that scattered cells with loose contacts. (*D*) Electron micrograph of a cluster of contacting GH cells stained with a GH antibody (labeled as GH). (*E*) Representative electron micrograph of a contact zone (arrow) between two GH cells. (*Inset*) Contact zones between GH cells stained with a β-catenin antibody (arrows).

performed two complementary statistical tests. First, a motif was detected when R mean was higher than a threshold level ($P < 0.001$). To determine the P value of the statistic, we computed the distribution of the statistic under the null hypothesis of independent R values. In a second test, we questioned whether a motif corresponded to a significant change between subsequent R means (ANOVA pair-wise test). We also classified the numbers of connected cell pairs within time windows ($P < 0.001$). When two groups of index windows were compared (two-sample t test, $P < 0.05$), we selected two subsequent periods of 30 min each [control + GH-releasing hormone (GHRH) exposure versus post-GHRH].

Results and Discussion

A Continuum of Connected GH Cells Wires the Whole Anterior Pituitary. Fixed GH-EGFP pituitaries from adult male GH-EGFP mice were imaged in serial steps to a depth of 200 μm from the pituitary capsule surface. It became apparent that almost all of the fluorescent (GH) cells were in close contact with other fluorescent cells, seeming to form a homotypic connected 3D cell continuum (Fig. 1A; see Movie 1, which is published as supporting information on the PNAS web site). This cell system consisted of numerous intercrossing strands of single GH cells, with larger clusters of GH cells positioned at the intersection of the strands (Fig. 1*B*). Pituitary-wide stacks of two-photon images were then collected for morphometric analysis in 3D, by using surface rendering of fluorescent voxels to reveal the extent of apposition of GH cells (Fig. 1*C*, $n = 5$). These data confirmed that all GH cells, even those that appear in random 2D sections as isolated cells or in small islets (2, 7), actually form a connected 3D multicellular GH cell system throughout the gland.

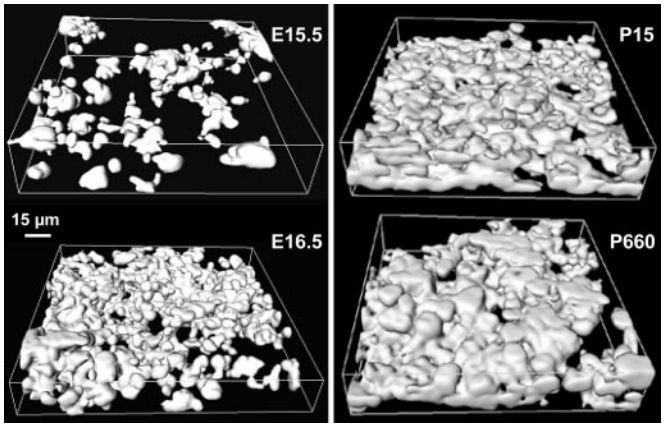

Fig. 2. Cell positioning continuously leads GH cells to form a cell continuum across the mouse's lifespan. Surface rendering of GH-GFP cell contours from two-photon image stacks of GH-GFP pituitaries. Animal ages are indicated on the right of 3D representations of GH cell positioning (E, embryos; P, postnatal).

Because GH cells in the pituitary gland make up the largest population of pituitary cells (7), some degree of homotypic apposition would be expected by chance and is not evidence *per se* of a tightly linked GH cell system. To address this question, we used a high-pressure, *in vivo* perfusion procedure to scatter cells with loose contacts and then examined those clusters of cells that remained in contact. After this procedure, both two-photon imaging of GH-GFP cells (data not shown) and immunoelectron microscopy of GH-positive cells (Fig. 1*D*, $n = 4$) showed that large portions of the GH system remained connected, with many homotypic GH cell assemblies that resisted disaggregation. These GH cell assemblies had closely apposed membrane contacts (Fig. 1*E*), with junctional complexes immunopositive for β-catenin, (Fig. 1*E Inset*, $n = 3$), suggesting that the strands and clusters of GH cells are linked with focal adherens junctions.

Robustness of the GH Cell System Across Lifespan. The distribution of GH cells was examined in pituitaries from GH-GFP mice over their lifespan. Once EGFP signals were detectable in the first few cells expressing GH in pituitaries during embryogenesis (12), 3D imaging uncovered organized strands of GH-EGFP cells (Fig. 2) (six of eight 15.5-day-old embryos). Then, a unique continuum of contacting GH cells forms within the parenchyma within 1 day (seven of seven 16.5-day-old embryos). This networking process coincides with the profound increase in both GH synthesis (13) and secretion (data not shown), and expression of GH secretagogue receptors at this age (14, 15). After birth, a unique ensemble of contacting GH cells was constantly observed in pituitaries until 24 months of age, thus suggesting that the presence of a GH cell continuum covers the whole lifespan of GH secretion (16).

Reversible Plasticity of the GH Cell System Architecture. We observed consistent differences in the GH cell strand and cluster densities in different regions of the gland and evident plasticity of the GH system architecture across lifespan. For example, in young adult (60-day-old) males, large GH cell clusters were much more prominent in the lateral zones of the gland, than in the median zone surrounding the stalk (Fig. 3*A*). Quantitative analysis of relative amount and density of GH cells in cell clusters versus cell strands in the lateral versus medial zones of each gland from groups of animals at different ages was performed by calculating the volume-

PHYSIOLOGY

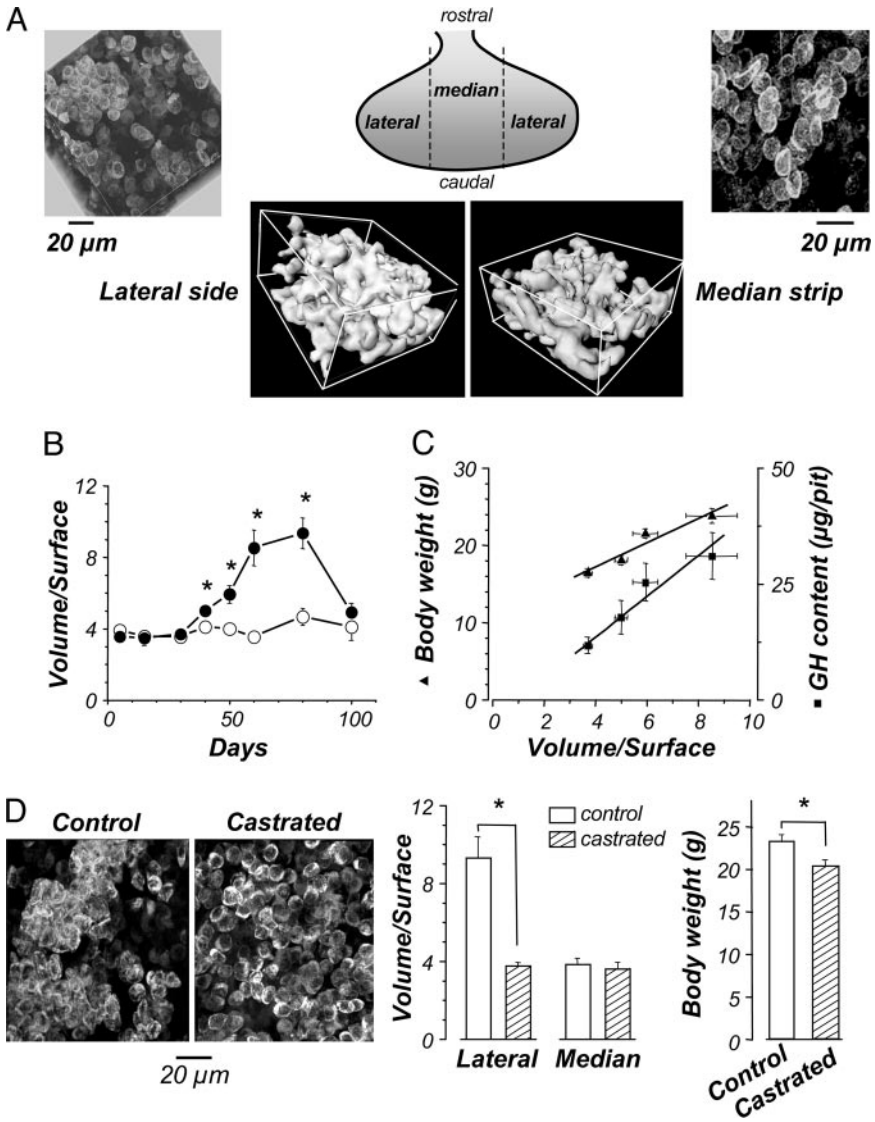

Fig. 3. Developmental modularity of the GH system architecture. (*A*) Shown are 3D reconstructions (*Upper*) and surface rendering views (*Lower*) of two-photon image stacks of the GH cell system architecture in both lateral (*Left*) and median (*Right*) regions of a 60-day-old male GH-EGFP pituitary. The calculated V/S ratios of surface rendering views in lateral and median zones were 7.7 and 3.8, respectively. (*B*) V/S ratios in both lateral (●) and median (○) regions vs. mice age. (*C*) V/S ratios in lateral regions (30- to 60-day-old males) vs. body weight (▲; linear regression: $y = 10.88 + 1.57x$, $R = 0.96$, $P = 0.04$) and GH content (■; linear regression: $y = 1.03 + 3.42x$, $R = 0.93$, $P = 0.03$). (*D*) (*Left*) Shown are 3D reconstructions of the GH system architecture in lateral regions of two 60-day-old males either sham-operated (control) or castrated at 15 days old. (*Center*) V/S ratios in both lateral and median regions from 60-day-old sham-operated (open columns) and castrated (hatched columns) male pituitaries. (*Right*) Body weights of 60-day-old sham-operated (open columns) and castrated (hatched columns) males. *, $P < 0.001$.

to-surface (V/S) ratios of the GH cell systems in each location. These results revealed that the geometry of the system varied markedly and reversibly from early postnatal life, through sexual maturation, to late adulthood (Fig. 3*B*). In prepubertal animals, the patterning of the GH cell system was similar in both zones, giving the same V/S ratios. From 30–80 days, the V/S ratio progressively increased in the lateral zones, whereas they remained constant in the median zone, indicating a marked increase in the proportion of GH cells in clusters in the lateral portions of the gland from puberty to adulthood. Interestingly, in the oldest mice examined (100-day-old), the V/S ratios returned toward prepubertal values in the lateral zones. Thus, the GH cell system is plastic, and its modification continues well into adulthood.

The increase in cluster density coincided with the process of sexual maturation and the increased activity of the GH axis known to occur at this time (17, 18). Remarkably, there was an excellent correlation of V/S ratio with body weight during the second month after birth, and between the onset of cell clustering, and of GH contents measured in pituitaries taken from other groups of age-matched mice (Fig. 3*C*). Furthermore, in a group of prepubertally castrated males, the decrease in growth rate after castration (Fig. 3*D*), possibly due to diminished GH pulsatility (19), was associated with a distinct remodeling of the GH cell system, resulting in a virtual absence of large GH cell clusters, but without a significant change in GH cell density in the lateral zones (51.2 ± 3.8% and 50.0 ± 1.6% in sham-operated and castrated mice, $n = 12$ and 10, respectively, $P > 0.05$) (Fig. 3*D*). Note that it is the geometry of the GH cell system, rather than the global cell density, that is organized in a way that would promote a more coordinated pulsatile release of GH that accelerates growth at puberty (4, 5). We suggest that intact GH clusters facilitate GH responses to secretagogues, because disaggregation of the GH system by enzymatic

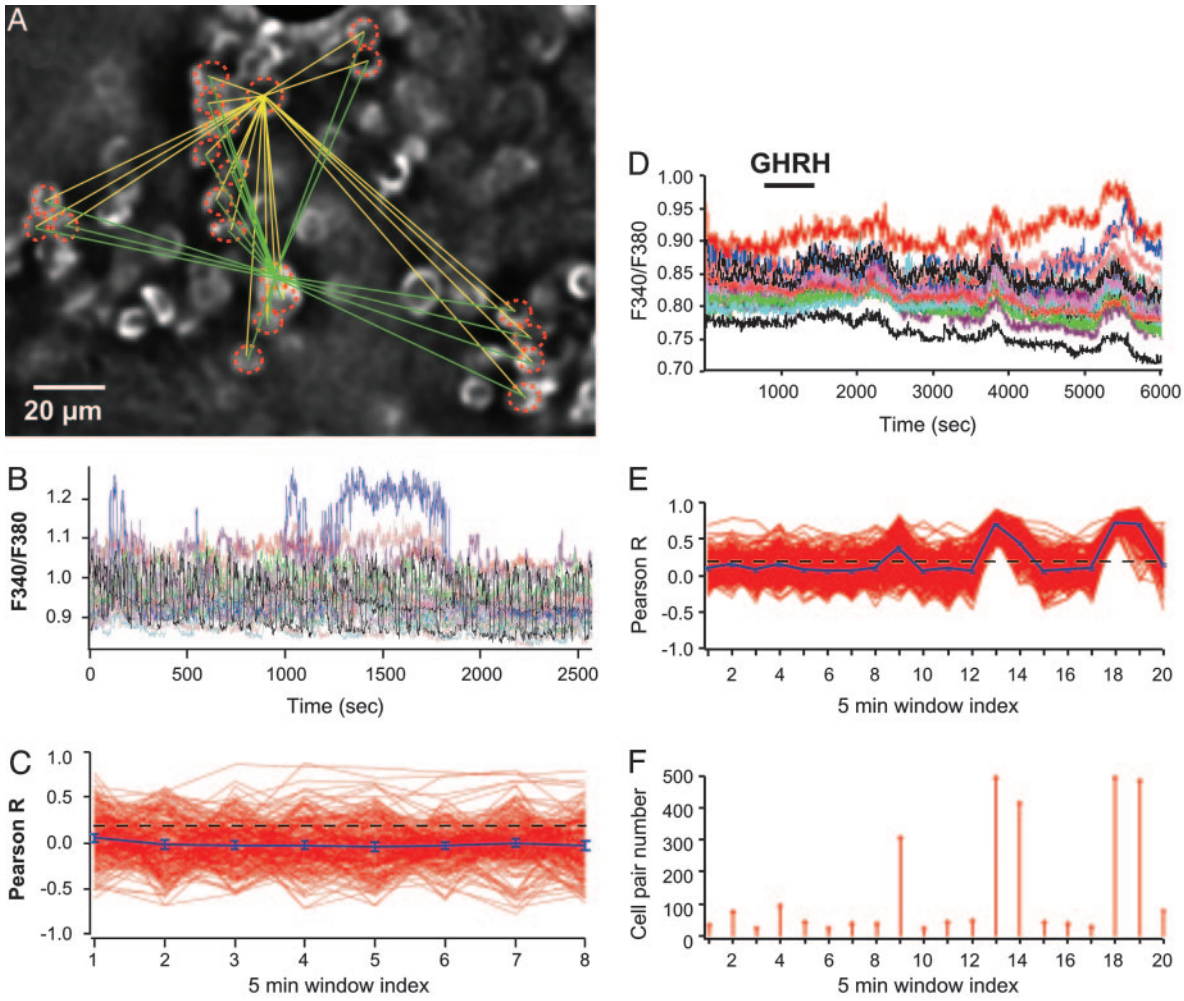

Fig. 4. GHRH triggers recurrent motifs of GH cell connectivity in the lateral zones. (*A*) Field of GH cells labeled with EGFP in the lateral zone. Only cells circled with a dashed line were also loaded with the fluorescent calcium dye fura-2. (*B*) Representative traces of spontaneous calcium spikes due to electrical activity. (*C*) Linear correlation (Pearson *R*) between calcium recordings among all cell pairs (C_1–C_2, C_1–C_3, . . . C_{N-1}–C_N) taken every 5 min. The yellow and green lines (*A*) illustrate the potent cell pairs for two recorded GH cells. Although some cell pairs displayed high *R* values, no large-scale cell connectivity ($P < 0.001$) was observed during spontaneous calcium spiking. (*D–F*) GHRH (10 nM) was applied during a 15-min time period (horizontal bar). (*D*) GHRH triggered a complex, oscillating calcium response in GH-EGFP cells recorded in the lateral zone. (*E*) Recurrent motifs of connectivity among large cell ensembles were observed in lateral regions ($P < 0.001$). (*F*) Distribution of numbers of connected cell pairs vs. time of calcium recording. GHRH triggered a delayed, cycling increase in connected cell pairs.

dispersion of mature male pituitaries led to a GH release response to GHRH 8-fold lower than that seen from large assemblies of GH cells preserved in pituitary slices (data not shown).

GHRH Switches on Recurrent Motifs of Cell Connectivity. To look for functional properties that may underlie the secretory efficiency of the GH system, we monitored cytosolic calcium concentration simultaneously in multiple identified GH cells. Calcium is a critical second messenger for hormone release (20) and is also involved in information transfer between connected cells in many cell ensembles (21, 22). Multicellular calcium recordings of GH-EGFP cells were performed in acute pituitary slices (Fig. 4 *A* and *B*). To quantify the strength of cell–cell connectivity between GH-GFP cells, the linear correlation (Pearson's *R* coefficient) was measured between all pairs of GH-EGFP cells loaded with fura-2. Subsequent 5-min-long segments of calcium recordings were analyzed as 5-min window index (Fig. 4*C*). Both the length (0.5–2 h) of calcium recordings and the time resolution of *R* measurements were chosen to approach the time range of pulses of GH release *in vivo*. In most experiments, GHRH, a selective GH cell agonist that controls the release of GH pulses *in vivo* (4, 5, 23, 24), was applied to fields of cells loaded with fura-2.

In control conditions, GH cells displayed calcium spikes that are due to spontaneous electrical activity (22, 25). Although some GH cell pairs displayed high *R* values, presumably due to local gap junction coupling (22), no large-scale cell connectivity was observed during spontaneous calcium spiking (Fig. 4*C*) ($P < 0.001$). However, a typical pattern of extended cell connectivity responses was prominent when GHRH was applied (15 min) in the lateral pituitary zones, which displayed large GH clusters in mature males. In six of eight fields, the overall number of cell pair connections increased in response to GHRH so that temporally precise calcium spike sequences recurred in synchrony several times; such recurring elements remained obvious, long after agonist application (Fig. 4 *D* and *E*). We also noted that the average periodicity of recurrent motifs of calcium signals detected in these lateral pituitary zones (28 min, $n = 16$) corresponded with the frequency of small GH pulses reported in simian pituitaries maintained *ex vivo* (26) and in pituitary cells that received a single pulse of GHRH (27). In the mouse pituitary, these wiring patterns that occurred again and again throughout the GH cell system were neither observed in long-lasting (≈2 h) recordings of spontaneous calcium activities without pituitary slice exposure to GHRH (six fields, data not

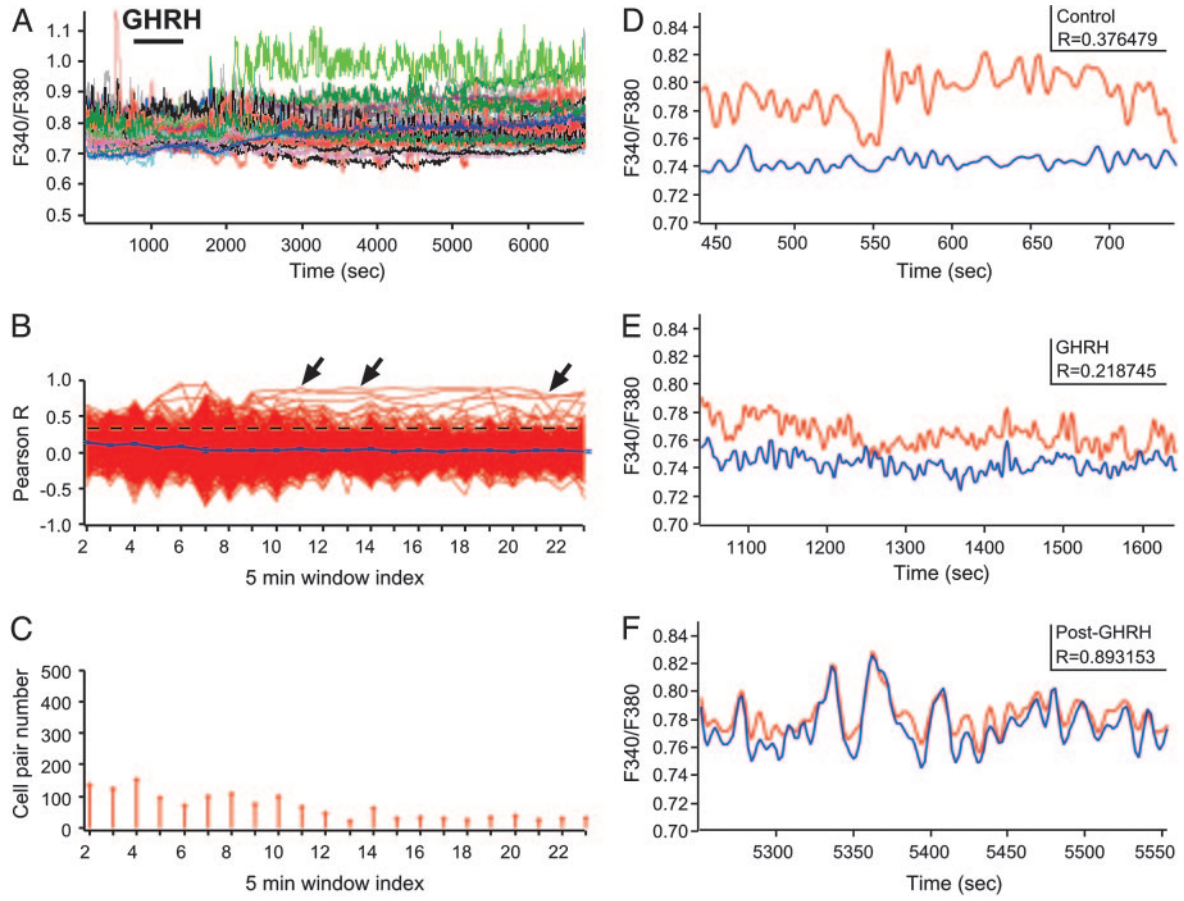

Fig. 5. GHRH triggers sustained changes in GH cell connectivity in the median zone. (*A–D*) GHRH (10 nM) was applied during a 15-min time period (horizontal bar). (*A*) GHRH triggered a prolonged change in calcium spiking activity. (B)Cross-correlation (Pearson *R*) between cell pairs. Arrows indicate cell pairs with high *R* values after GHRH application ($P < 0.001$). (*C*) Numbers of cell pairs with significant cell connectivity ($P < 0.001$). Paradoxically, GHRH also caused a delayed decrease in the numbers of connected cell pairs ($P < 0.05$). (*D–F*) Changes in both calcium spike firing and cell connectivity (Pearson *R*) in a pair of neighboring GH cells before (*D*), during (*E*), and after (*F*) GHRH application. The cell pair corresponded to a trace marked by an arrow in *B*.

shown, $P > 0.05$) nor in GHRH-stimulated GH cells that were dispersed after enzymatic dispersion of lateral pituitary portions (five fields, data not shown, $P > 0.05$). These recurring motifs of cell connectivity most likely reflect the predominant response of the GH cell system when a pulse of hypothalamic GHRH invades the gland because the majority of GH cells (≥80%) are located in the lateral pituitary regions.

GHRH Changes in GH Cell Connectivity Are Spatially Stereotyped. A distinct GHRH-evoked change in cell connectivity was detected in the median pituitary zone. GHRH triggered a profound and sustained stimulation of calcium spiking (Fig. 5*A*) that was associated with a selective increase in cell connectivity between pairs or triplets of neighboring GH-EGFP cells (Fig. 5*B*). An example of a responsive cell doublet is illustrated in Fig. 5 *D–F* where the increase in cell connectivity (Fig. 5*F*) followed an initial rise in calcium spike frequency (Fig. 5*E*). This result showed in pituitary cells that an agonist triggered both intracellular and intercellular communication mechanisms with different timescales. Surprisingly, the overall number of cell pair connections markedly decreased after GHRH stimulation (Fig. 5 *B* and *C*, four of seven different fields, $P < 0.05$). These results suggest that GHRH does not simply affect all cells independently in this region but changes the local pattern of cell–cell communication, resulting in small islets of more highly functionally connected GH cells at some points in the system, interspersed with functionally less connected GH cells. This paradoxical reduction would "sharpen" the global pulsatile response by minimizing the contribution of less coordinated cell assemblies within the network. Note that the GHRH responses were markedly different in the median zone in comparison with those observed in the lateral zones, indicating that GHRH triggered spatially stereotyped motifs of cell connectivity, which clearly depend on the local geometry of the GH system architecture within different regions of the gland.

GH Cells Form a Functional Cell Network. This combined morphological and functional analysis of the entire GH population in 3D shows that GH cells actually form a connected homotypic structure that pervades the entire gland. This structure exhibits three of the most shared principles of biological networks (28): robustness of GH network architecture across a mouse's lifetime, modularity of cell positioning (which varies with activity in the GH axis and body growth), and spatially localized patterns of cell–cell communication showing recurring responses to specific stimuli for GH release. Therefore, our results provide strong evidence that GH cells function as a geometry-driven network of cells, connected to each other by adherens junctions.

Moving the focus from single-cell function to whole-organ function is crucial to understanding function at the systems biology level. It is particularly obvious for GH secretion, which clearly requires a high degree of coordination of a large population of individual GH cells to generate a large secretory burst into the blood stream that survives dilution and mixing in the circulation, to deliver a defined pulsatile signal to peripheral tissues (4, 24, 29–31). The conven-

tional view of this process is that cell numbers and cell activities can be considered independent responsive elements, with the output some population (e.g., Gaussian) distribution response. However, it probably arises from a 2D view that has missed the higher level organizational properties of the entire GH cell population. We now show that the apparently dispersed secretory elements of the GH system are actually organized to form a structurally and functionally interdependent network and suggest that the proper functioning of the GH cell population depends on the fine tuning of an "N.A.P." triplet involving the number, activity, and positioning of GH cells. This N.A.P. triplet functioning allows for fine tuning of communication mechanisms (22, 32) between large numbers of connected GH cells within a network to produce rapid and synchronized hormone pulses in response to physiological needs.

Networks of Endocrine Cells: Perspectives. Because the GH cell network is plastic and the numbers of GH cells change with physiological demands, there must be mechanisms to replace dying GH cells and to ensure that their replacements find their proper place in the network. Failure of these mechanisms, as in developmental or pathological disruption of the network architecture, may have important deleterious consequences for GH responses. Preliminary observations of the GH network in mice with GH cell hypoplasia and dwarfism showed spatially localized "broken" branches of GH cells [i.e., decrease in network robustness (data not shown)], and the breakdown of GH cell organization in 2D is well described in pituitary tumor pathologies associated with dysregulated GH secretion (2). Therefore, our 3D approach to functional analysis of the GH network could have importance in human pituitary pathophysiology. One can imagine that the development of noninvasive imaging of the present 3D network [e.g., with selective ligands for GH cells for positron-emission tomography (PET) scans] (33) might be useful in diagnosis of some gradually developing GH-deficiency states, such as those after traumatic brain injury (34, 35) or cranial irradiation (36). GH cell network disruption could well contribute to the uncoordinated GH profiles seen in GHD subjects otherwise described as exhibiting "neurosecretory dysfunction."

The combined transgenic, morphological, and functional imaging approaches, used to define the GH cell network characteristics, could readily be applied to other cell types currently thought of as "heterogeneously distributed," not least to other endocrine cell types in the pituitary, and to examine their relationship with other non-endocrine cell types, such as the folliculostellate cell network already described in the pituitary (37). Moreover, transgenic mice that express fluorescent proteins in other pituitary cell types such as POMC (38) or PRL (I.C.A.F.R. and P. R. Le Tissier, unpublished results) offer similar opportunities to address whether cell networking is a prerequisite for the build-up of large hormone pulses that occur in other systems and over different timescales. For example, one might consider the role of large-scale cell network organization for corticotropin (ACTH) (39) and luteinizing hormone (LH) systems (40).

Endocrine pituitary cells belong to the widespread "diffuse endocrine system," which was first described ≈70 years ago in 2D histological studies (41, 42). Taking a 3D view of other members of the diffuse endocrine system should reveal organizational features that may be beneficial for their normal function (e.g., how ghrelin cells in the stomach and GI tract coordinate their function) (43), or may be deleterious in dysfunction (e.g., newly formed neuroendocrine cell foci detected among some common cancers) (44, 45). How such homotypic networks assemble during embryonic development and are maintained through normal cell turnover and replacement can now be studied by using the approaches described here.

We thank Annie Delalbre, Anne Cohen-Solal, Dominique Haddou, Alain Carrette, and Philippe Didier for their invaluable assistance. This work was supported by grants from Institut National de la Santé et de la Recherche Médicale, Centre National de la Recherche Scientifique, the Medical Research Council (United Kingdom), the National Institutes of Health, the European Community, Ministère de la Recherche (ACI-France), Fondation Simone Del Duca, Fondation pour Recherches Médicales, and Région Languedoc-Roussillon.

1. Kostyo, J. L. & Goodman, H. M. (1999) *Hormonal Control of Growth* (Oxford Univ. Press, Oxford).
2. Asa, S. L. & Ezzat, S. (2002) *Nat. Rev. Cancer* **2,** 836–849.
3. Bowers, C. Y., Reynolds, G. A., Durham, D., Barrera, C. M., Pezzoli, S. S. & Thorner, M. O. (1990) *J. Clin. Endocrinol. Metab.* **70,** 975–982.
4. Clarke, R. G. & Robinson, I. C. A. F. (1985) *Nature* **106,** 281–289.
5. Tannenbaum, G. S. & Martin, J. B. (1976) *Endocrinology* **98,** 562–570.
6. Sartor, O., Bowers, C. Y. & Chang, D. (1985) *Endocrinology* **116,** 952–957.
7. Baker, B. L. (1974) *Handbook Physiol. Sect. Endocrinol.* **4,** 45–80.
8. Denk, W., Delaney, K. R., Gelperin, A., Kleinfeld, D., Strowbridge, B. W., Tank, D. W. & Yuste, R. (1994) *J. Neurosci. Methods* **54,** 151–162.
9. Fauquier, T., Lacampagne, A., Travo, P., Bauer, K. & Mollard, P. (2002) *Trends Endocrinol. Metab.* **13,** 304–309.
10. Alonso, G., Runquist, M., Hussy, N., Duvoid, A. & Moos, F. (2003) *Eur. J. Neurosci.* **18,** 1889–1903.
11. Magoulas, C., McGuinness, L., Balthasar, N., Carmignac, D. F., Sesay, A. K., Mathers, K. E., Christian, H., Candei, L., Bonnefont, X., Mollard, P. & Robinson, I. C. (2000) *Endocrinology* **141,** 4681–4689.
12. Dasen, J. S. & Rosenfeld, M. G. (2001) *Annu. Rev. Neurosci.* **24,** 327–355.
13. Slabaugh, M. B., Lieberman, M. E., Rutledge, J. J. & Gorski, J. (1982) *Endocrinology* **110,** 1489–1497.
14. Gage, P. J., Lossie, A. C., Scarlett, L. M., Lloyd, R. V. & Camper, S. A. (1995) *Endocrinology* **136,** 1161–1167.
15. Lin, S. C., Lin, C. R., Gukovsky, I., Lusis, A. J., Sawchenko, P. E. & Rosenfeld, M. G. (1993) *Nature* **364,** 208–213.
16. Robinson, I. C. A. F. & Hindmarsh, P. C. (1999) in *Hormonal Control of Growth*, eds. Kostyo, J. L. & Goodman, H. M. (Oxford Univ. Press for the Am. Physiol. Soc., New York), pp. 329–396.
17. Pincus, S. M., Gevers, E. F., Robinson, I. C., van den Berg, G., Roelfsema, F., Hartman, M. L. & Veldhuis, J. D. (1996) *Am. J. Physiol.* **270,** E107–E115.
18. Pincus, S. M., Veldhuis, J. D. & Rogol, A. D. (2000) *Am. J. Physiol.* **279,** E417–E424.
19. Jansson, J. O., Eden, S. & Isaksson, O. G. P. (1985) *Endocr. Rev.* **6,** 128–150.
20. Neher, E. & Zucker, R. S. (1993) *Neuron* **10,** 21–30.
21. Berridge, M. J., Lipp, P. & Bootman, M. D. (2000) *Nat. Rev. Mol. Cell Biol.* **1,** 11–21.
22. Guérineau, N. C., Bonnefont, X., Stoeckel, L. & Mollard, P. (1998) *J. Biol. Chem.* **273,** 10389–10395.
23. Brazeau, P., Ling, N., Bohlen, P., Esch, F., Ying, S. Y. & Guillemin, R. (1982) *Proc. Natl. Acad. Sci. USA* **79,** 7909–7913.
24. Plotsky, P. M. & Vale, W. (1985) *Science* **230,** 461–463.
25. Schlegel, W., Winiger, B. P., Mollard, P., Vacher, P., Wuarin, F., Zahnd, G. R., Wollheim, C. B. & Dufy, B. (1987) *Nature* **329,** 719–721.
26. Stewart, J. K., Clifton, D. K., Koerker, D. J., Rogol, A. D., Jaffe, T. & Goodner, C. J. (1985) *Endocrinology* **116,** 1–5.
27. Guillemin, R. C., Brazeau, P., Briskin, A. & Mandell, A. J. (1983) in *Synergetics of Brain*, eds. Basar, E., Flohr, H., Haken, H. & Mandell, A. J. (Springer, New York), pp. 155–162.
28. Alon, U. (2003) *Science* **301,** 1866–1867.
29. Hartman, M. L., Veldhuis, J. D. & Thorner, M. O. (1993) *Horm. Res.* **40,** 37–47.
30. Tannenbaum, G. S., Choi, H. K., Gurd, W. & Waxman, D. J. (2001) *Endocrinology* **142,** 4599–4606.
31. Clark, R. G., Chambers, G., Lewin, J. & Robinson, I. C. (1986) *J. Endocrinol.* **111,** 27–35.
32. Rubinek, T., Yu, R., Hadani, M., Barkai, G., Nass, D., Melmed, S. & Shimon, I. (2003) *J. Clin. Endocrinol. Metab.* **88,** 3724–3730.
33. Sweet, I. R., Cook, D. L., Lernmark, A., Greenbaum, C. J. & Krohn, K. A. (2004) *Diabetes Technol. Ther.* **6,** 652–659.
34. Agha, A., Rogers, B., Sherlock, M., O'Kelly, P., Tormey, W., Phillips, J. & Thompson, C. J. (2004) *J. Clin. Endocrinol. Metab.* **89,** 4929–4936.
35. Aimaretti, G., Ambrosio, M. R., Di Somma, C., Fusco, A., Cannavo, S., Gasperi, M., Scaroni, C., De Marinis, L., Benvenga, S., degli Uberti, E. C., *et al.* (2004) *Clin. Endocrinol.* **61,** 320–326.
36. Gleeson, H. K. & Shalet, S. M. (2004) *Endocr. Relat. Cancer* **11,** 589–602.
37. Fauquier, T., Guérineau, N. C., McKinney, R. A., Bauer, K. & Mollard, P. (2001) *Proc. Natl. Acad. Sci. USA* **98,** 8891–8896.
38. Cowley, M. A., Smart, J. L., Rubinstein, M., Cerdan, M. G., Diano, S., Horvath, T. L., Cone, R. D. & Low, M. J. (2001) *Nature* **411,** 480–484.
39. Young, E. A., Abelson, J. & Lightman, S. L. (2004) *Front. Neuroendocrinol.* **25,** 69–76.
40. Veldhuis, J. D. (2000). *Novartis Found. Symp.* **227, 163–185**; discussion 185–189.
41. Feyrter, F. (1938) *Über Diffuse Endokrine Epitheliale Organe* (J. A. Barth, Leipzig, Germany).
42. Pearse, A. G. & Takor, T. T. (1976) *Clin. Endocrinol. (Oxford)* **5,** Suppl., 229S–244S.
43. Kojima, M., Hosoda, H., Date, Y., Nakazato, M., Matsuo, H. & Kangawa, K. (1999) *Nature* **402,** 656–660.
44. Garabedian, E. M., Humphrey, P. A. & Gordon, J. I. (1998) *Proc. Natl. Acad. Sci. USA* **95,** 15382–15387.
45. Wick, M. R. (2000) *Am. J. Clin. Pathol.* **113,** 331–335.